We are IntechOpen, the world's leading publisher of Open Access books Built by scientists, for scientists

4,800
Open access books available

122,000
International authors and editors

135M
Downloads

Our authors are among the

154
Countries delivered to

TOP 1%
most cited scientists

12.2%
Contributors from top 500 universities

CLARIVATE ANALYTICS BOOK CITATION INDEX INDEXED

WEB OF SCIENCE™

Selection of our books indexed in the Book Citation Index in Web of Science™ Core Collection (BKCI)

Interested in publishing with us?
Contact book.department@intechopen.com

Numbers displayed above are based on latest data collected.
For more information visit www.intechopen.com

Chapter

Synthesis, Characterization, and Adsorption Properties of Nanoporous Materials

Rolando Roque-Malherbe and Carlos de las Pozas del Rio

Abstract

During the last years, the authors have synthesized, characterized, and studied the adsorption properties of nitroprussides, Prussian blue analogues, akaganeites, MeAPOs, metal–organic frameworks, and extremely high specific surface amorphous silica, which allowed the storage of about 11 wt.% of hydrogen in the form of ammonia. In this sense, using the solid-state reaction method, sol–gel methodologies, together with aluminosilicate, high silica and non-aluminosilicate zeolite synthesis methods, were described, moreover was explained how to prepare active carbons along with the synthesis of Prussian blue analogues (PBAs) and nitroprussides (NPs). In addition, the characterization of the materials of interest applying X-ray diffraction, thermogravimetric analysis, DRIFTS, and room-temperature Mossbauer spectrometry was discussed. Besides, the concepts that define physical adsorption and examples of adsorption data, which were tested with the help of the Dubinin, osmotic adsorption and Langmuir-type isotherms, were defined. Later, the methodology was described for the measurement of adsorption data with the help of the volumetric method. Moreover, a description of the thermodynamics of adsorption, along with the methodology for the calculation of calorimetric data with the help of heat flow calorimeters together with the measurement of differential heats of adsorption data was developed. Finally, the different interaction forces that make possible adsorption were discussed.

Keywords: physical adsorption, isotherms, Dubinin and osmotic tests, differential heats of adsorption, nitroprussides, Prussian blue analogues, silica and natural zeolites

1. Introduction

The concept of "adsorption" was recommended by Kayser in 1881 to explain the growth in concentration of gas molecules on the adjacent surface of a solid adsorbent, an effect previously noted by Fontana and Scheele in 1777 [1]. In particular, majority of adsorbents useful for industrial applications have pores with hole dimensions in the nanometer region; in this pore-size zone, adsorption is on the one hand a significant methodology for the characterization of porous materials; to be exact, gas adsorption offers evidence concerning the mesopore area, volume and size of the pores together with the energetics of adsorption [2]. Also, gas adsorption is a vital unitary operation for sustainable energy and pollution abatement

applications of nanoporous materials along with the industrial uses, where materials like metal organic framework molecular sieves, metal organic frameworks, Prussian blue analogues, mesoporous molecular sieves, pillared clays, silica, alumina, active carbons, titanium dioxides, magnesium oxides, carbon nanotubes together with zeolites and related materials are the most widely studied and applied adsorbents in Science and Technology [3].

In addition to their adsorption properties, nanoporous materials are a group of advanced materials with other excellent properties and applications in many fields, for example, waste water treatment [4–6], ionic conduction [7], ionic exchange [8], gas separation [9], membranes [10], catalysts [11], catalyst supports [12] and detergency [13].

The classification of the different pore widths of porous adsorbents was carried out by the International Union of Pure and Applied Chemistry (IUPAC); in this classification, adsorbent materials are categorized as those with pore diameters greater than 50 nm, named macroporous adsorbents, while mesoporous materials show pore diameters between 2 and 50 nm that are termed microporous; those adsorbents showing pore diameters between 0.3 and 2 nm, where, the pore width, *Dp,* is defined as equal to the diameter in the case of cylindrical shaped pores, and as the distance between opposite walls in the case of slit-shaped pores [14].

In addition, the clean surface of an adsorbent is characterized by the fact that the atoms that produce the surface have non-saturated bonds, fact producing an adsorption field above this surface; been the adsorption field the cause of the formation of a stockpile of molecules close to the adsorbent surface; this effect, i.e., adsorption, is a universal propensity of surface systems, given that throughout this process a reduction of the surface tension is experienced by the solid; been, adsorption the term applied to describe this process; whereas for the opposite, the term desorption is used [1].

Now it is necessary to state that the occupation of the adsorption space by adsorbed molecules in complex porous systems occurs roughly in the following form: initially, micropore filling takes place, with the adsorption process being controlled almost totally by the interaction of the adsorbed molecules with the pore walls; thereafter, at higher pressures, the external surface is covered, which is a monolayer and a multilayer adsorption on the walls of mesopores, and open macropores take place. Finally, capillary condensation occurs in the mesopores [2]. On the other hand, dynamic adsorption is a mass transfer between a mobile, solid, or liquid phase, and the adsorption bed packed in a reactor, been necessary to carry out the dynamic adsorption, a reactor, where the adsorption process will occur in the reactor adsorbent packed bed, been, the adsorbents normally used for these applications are active carbons, zeolites and related materials, silica, mesoporous molecular sieves, alumina, titanium dioxide, magnesium oxide, clays, and pillared clays [3].

2. Synthesis

2.1 Solid-state reaction method

Inorganic compounds are mixed, following stoichiometric proportions; after that, the powders are thoroughly milled and then finally thermally treated to get the required product, been, perovskites synthesized using this method [15, 16].

2.2 Sol-gel methodologies

These processes can be based on the hydrolysis condensation of metal alkoxides. In the important case of amorphous silica synthesis, silicic acid is first produced by

the hydrolysis of a silicon alkoxide, formally a silicic acid ether; then, the global reaction continues as a condensation polymerization to form high molecular weight polysilicates, which connect together to produce a gel [17].

2.3 Aluminosilicate zeolites

These materials are normally synthesized in hydrothermal conditions using solutions that are composed of sodium hydroxide, sodium silicate and sodium aluminate, where three steps are observed during the synthesis process, i.e., induction, nucleation, and crystallization, which determine the specific zeolite produced by the applied reactants, along with the parameters used, such as temperature, pH, and time [18, 19].

2.4 High silica and non-aluminosilicate zeolites

In this case, the aluminosilicate synthesis is complemented with the addition of structure-directing agents (SDA), such as quaternary ammonium cations, linear or cyclic ethers, and coordination compounds. been, the first high-silica zeolites, that is, ETA, EU, NU, and the ZSM series, patented in the late 1960s, or early 1980s [20]; moreover, high silica zeolite can be as well synthesized using ethanol and seeds of the desired phase [21]; meanwhile, Microporous aluminophosphate molecular sieves, that is, non-aluminosilicate zeolites; such as: SAPO molecular sieves were obtained by incorporation of Si in the AlPO framework, while MeAPO molecular sieves are obtained by the inclusion of Ga, Be, Va, Co, Fe, Mg, Mn, Zn in the AlPO framework obtaining between others: gallophosphates, zincophosphates, beryllophosphates, vanadophosphates and ferrophosphates [22].

Active Carbon prepared with wood, lignite, peat, coconut, eucalyptus lignin, and apricot, cherry and olive stones under physical (a) and chemical activation (b) methods; i.e. [23–25]:

a. carbonization at 800–1000°C under inert gas, and activation under oxidizing agents, as a rule, carbon dioxide or water vapor.

b. chemical activation requires a treatment with: sulfuric acid, phosphoric acid, zinc chloride, potassium hydroxide at 400–1000°C, followed by the elimination of the dehydrating agent by meticulous washing.

Prussian blue analogues (PBAs) [26, 27] and nitroprussides (NPs) [28] are produced by mixing solutions of $K_3[Fe(CN)_6]$, for the synthesis of Prussian blue analogues, and $Na_2[Fe(CN)_5NO]$ for the synthesis of nitroprussides with a nitrate of the corresponding metal to get the corresponding PBAs and NPs.

3. Characterization

The X-ray Diffraction (XRD) methodology was used to determine the crystalline phases present in the natural and synthesized materials, together with the investigation of the nucleation and growth process during the synthesis of different materials to be used as adsorbents, ion exchangers and catalysts [29]. The XRD tests were carried out, at room temperature using a stage similar to an Anton Paar HTK-1200 N with an equipment similar to a Bruker D8 Advance system in a Bragg-Brentano vertical goniometer configuration, the angular measurements being made applying steps of 0.01° from 5 to 80°, using a Cu anode tube together with a Ni filter

placed, prior to the detector, to eliminate Cu K_α radiation the one-dimensional detector was employed [26].

3.1 Thermo-gravimetric analysis (TGA)

The analytical test was carried out with an equipment similar to a TA, Q-500 instrument; the samples were placed onto a ceramic sample holder suspended from an analytical balance, suspended from an analytical balance; then the temperature was linearly scanned, from 25 to 300 C, at a heating rate of 5 C/min under a pure N_2 flow of 100 mL/min. TGA testing process was carried out with a TA, Q-500 instrument, and the samples were placed onto a ceramic sample holder [27].

DRIFTS were gathered using equipment similar to a Thermo Scientific Nicolet iS10 FTIR spectrometer. The data of the hydrated and dehydrated samples were collected at a resolution of 4 cm^{-1} employing 100 scans per sample; a background, with pure KBr, was in all cases collected before the collection of the spectra. Both the hydrated and dehydrated samples were gathered at room temperature while flowing N_2 (Praxair, 99.99%) at a rate of 50 cc/min; while, the dehydration of the studied samples was performed at 100°C for 2 h in N_2 flow of 50 mL/min while the sample under test was included in the finger-sample-holder of the IR high temperature cell [28].

Room-temperature Mossbauer Spectrometry measurements were made with a system similar to a SEECo supplied spectrometer operating at constant acceleration mode with a 50 mCi ^{57}Co γ-ray source in a Rh matrix made by Rietverc GmbH. The 1024-point raw data were folded and analyzed using WMOSS, a public domain Mossbauer spectral analysis program; the calibration was made with reference to α-Fe metal [30].

4. Definition and terms

4.1 Adsorption isotherm

It is the most important measurement made to characterize an adsorbent; it is defined as the relationship between the amount adsorbed, n_a, and the equilibrium pressure, P, at constant temperature, T [1, 2] (**Figure 1**)

$$n_a = f(P)_T \tag{1}$$

4.2 Physical and chemical adsorption

The gas adsorption process is normally considered a physical process, named physical adsorption, since the molecular forces involved in this process are usually of the van der Waals type. Meanwhile Chemical adsorption of gases in solid surfaces takes place in the case where during the adsorption process a reaction with exchange of electrons between the solid surface and the gas molecules with the formation of chemical bonds takes place, been, the adsorbent the solid phase and the adsorbate the gas phase [14].

4.3 Mobile and immobile adsorptions

Gas and vapor adsorption in solid adsorbents can be also classified as mobile adsorption, where the first case occurs when the adsorbed molecule is performed as

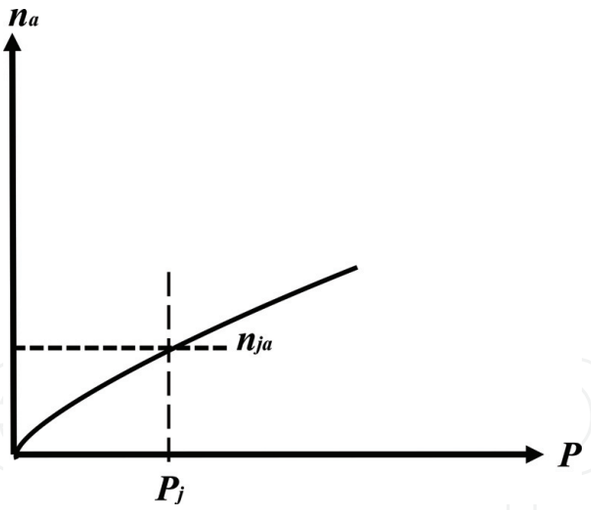

Figure 1.
Graphic representation of the adsorption isotherm.

a gas molecule is free to move within the adsorption space, or the instance of immobile adsorption, taking place in the case where the adsorbed molecule vibrates around an adsorption site [2, 3].

4.4 Monolayers and multilayers

For open surfaces, adsorption consists of a layer-by-layer loading process, where the first layer is filled as in the case when $\theta = \frac{n_a}{N_m} = 1$, where θ is the surface recovery and N_m is the monolayer capacity; as a result, it is understood that we have monolayer adsorption when $\theta < 1$ and multiplayer adsorption when $\theta > 1$ [31].

4.5 Porous adsorbents

They are characterized by their specific surface area, denoted by S, and measured in (m^2/g), in which the surface area is the outer surface, concretely, the area external to the micropores. If the adsorbents do not have micropores, the surface area and the outer surface area match; furthermore, the micropore volume is represented by W_{MP}, measured in (cm^3/g), whereas the total pore volume labeled W is the sum of the micropores and mesopore volumes [32] of the adsorbent, also measured in (cm^3/g). Lastly, we have the pore size distribution (PSD), i.e., a plot of $\frac{\Delta v_P}{\Delta D_p}$ versus *Dp*, where Vp is the pore volume accumulated up to the pore width *Dp* measured in (cc-STP/g Å) [26, 27]. Now it is necessary to state that cc-STP is a unit denoting the amount adsorbed, measured in cubic centimeters at standard temperature and pressure (STP), that is, 273.15 K and 760 Torr, that is, 1.01325×10^5 Pa.

4.6 Magnitude of adsorption

The interfacial layer is the non-homogeneous section of an adsorption system, i.e., between two neighboring bulk phases (**Figure 2**), where the properties typifying this region are radically dissimilar from, but associated to, the properties of the bulk phases; in which, to deal with this system is assumed that in the ideal reference system, the concentration must be constant up to the Gibbs dividing surface (GDS) (see **Figure 2**); been, in an actual system [32]

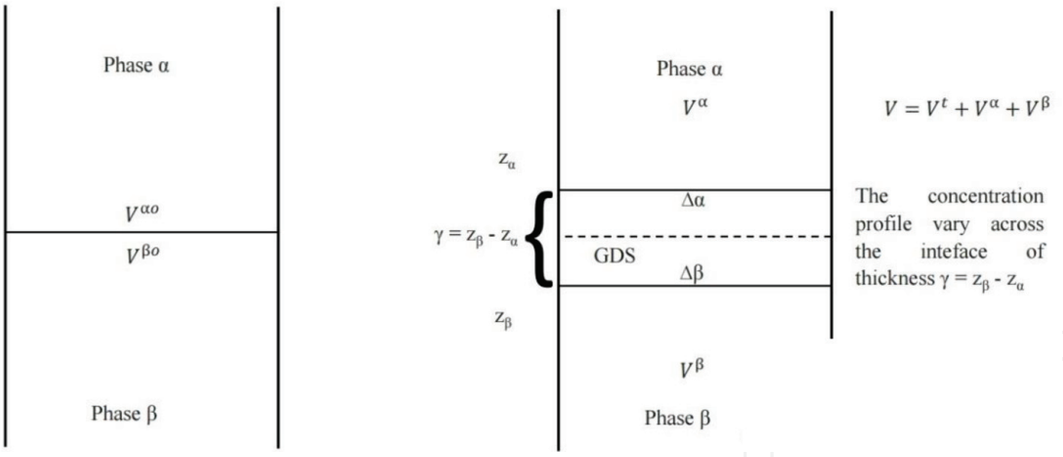

Figure 2.
Gibbs dividing surface.

$$n^a = \int_0^{V^a} cdV = \int_0^t cdz \tag{2}$$
$$V^{\propto} = At$$

Then the total amount of gas molecules in the system measured in (mol/g) is

$$n = n^a + V^g c_g^g$$
$$n^a = n - V^g c_g^g$$

where

$V^{\propto}$ is the volume of the adsorption space, V^g is the volume of the gas phase, c_g^g is the concentration of the gas phase, c_s^g is the concentration of the gas in the solid phase, A is the adsorbent surface area, t is the thickness of the surface layer, and n is the total amount of gas molecules in the system.

Finally the isotherm is calculated as follows:

$$n_a = \frac{n^a}{m_s} = F(P)_T$$

where m_s is the degassed adsorbent mass in grams. Then if the ideal gas equation is applied,

$$\mathrm{PV} = \mathrm{nRT} \tag{3}$$

Been, n and T, kept constants, then [29]:

$$\mathrm{P_i V_i} = \mathrm{P_j V_j} = \mathrm{nRT} = \mathrm{const} \tag{4}$$

where P is the pressure in atmosphere, V is the volume in milliliters;
$1\ \mathrm{ml} = 1\ \mathrm{cm}^3 = 10^3\mathrm{mm}^3 = 10^{-3}\mathrm{dm}^3 = 10^{-3}\mathrm{l}$, n is the number of gas moles, T is the temperature in kelvin (K), and R is the gas constant.

Thereafter, using Eq. (4), based in the scheme of the volumetric adsorption equipment shown in **Figure 11**, we get:

$$\mathrm{P}_{at}\mathrm{V_m} = \mathrm{P_i}(\mathrm{V_m} + \mathrm{V_d} + \mathrm{V_x}) \tag{5}$$
$$\mathrm{P}_{at} = 2l_{at}$$

In **Figure 11**, a schematic representation of volumetric gas adsorption measurement equipment is shown, where using the scheme, it is possible to show that:

$$V_x = \pi r^2 \left(X_i' + l_0\right) \tag{6}$$
$$\left(X_i' + l_0\right) = X_i$$

Initially V_m is filled with air and then the valves are opened allowing air up to equilibrium with the atmospheric pressure of the room, which can be measured with a barometer; now given that V_m was calibrated, filling it with water, then X_i allow us to calculate:

$$P_i[\text{mmHg}] = 2X_i[\text{mmHg}]$$
$$P_{at} = 2l_{at}[\text{mmHg}]$$

where P_{at} is the atmospheric pressure and P_1 is the measurement of pressure after expansion.

Substituting Eq. (6) on (5), the dose volume is calculated as:

$$V_d = \frac{l_{at}}{X_i} V_m - \left(V_m + \pi r^2 X_i\right)$$

In this sense, using the proportions rule, we get:

$$\frac{2X_i[\text{mmHg}]\text{x}1[\text{Atm}]}{760[\text{mmHg}]} = P_i[\text{Atm}]$$

Consequently applying the ideal gas law:

$$P_i[\text{Atm}]\left(2\pi r^2 X_i\left[\text{mm}^3\right]\text{x}10^3 + V_d[\text{ml}]\right) = n_i[\text{mmol}]R\left[\frac{\text{atm.ml}}{\text{mmol.K}}\right]T[\text{K}]$$

where

$$\frac{P_i[\text{Atm}]\left(2\pi r^2 X_i[\text{mm}^3]\text{x}10^3 + V_d[\text{ml}]\right)}{R\left[\frac{\text{atm.ml}}{\text{mmol.K}}\right]T[\text{K}]} = n_i[\text{mmol}]$$

Number of moles in the dose volume and the volume provided by the displacement of the manometer.

5. Experimental determination of V_a and V_a' and the numbers of mole gas adsorbed n_{aj}

When the valve of the sample holder is opened, the gas is expanded; hence:

$$\frac{P_i[\text{Atm}]\left(2\pi r^2 X_i[\text{mm}^3]\text{x}10^3 + V_d[\text{ml}]\right)}{R\left[\frac{\text{atm.ml}}{\text{mmol.K}}\right]T[\text{K}]} = \frac{P_j[\text{Atm}]\left(2\pi r^2 X_j[\text{mm}^3]\text{x}10^3 + V_d[\text{ml}] + V_a\right)}{R\left[\frac{\text{atm.ml}}{\text{mmol.K}}\right]T[\text{K}]} = n_i$$

where:

$$\frac{P_j}{P_i}[\text{Atm}]\left(2\pi r^2 X_j\left[\text{mm}^3\right]\text{x}10^3 + V_d[\text{ml}] + V_a\right) - [\text{Atm}]\left(2\pi r^2 X_i\left[\text{mm}^3\right]\text{x}10^3 + V_d[\text{ml}]\right) = V_a$$

This allows the calculation of Va, the so-called dead volume. Nevertheless the really expanded volume should consider the volume occupied by the adsorbent sample, i.e.:

$$V_{muestra}\left[cm^3\right] = \frac{m[g]}{\rho\left[\frac{g}{cm^3}\right]}$$

And ρ is the apparent density of the tested adsorbent material. Consequently:

$$V_a - V_{muestra} = V'_a$$

According ideal gas low:

$$\frac{P_i[Atm]\left(2\pi r^2 X_i[mm^3]x10^3 + V_d[ml]\right) + P_{j-1}V'_a}{R\left[\frac{atm.ml}{mmol.K}\right]T[K]} - \frac{P_j[Atm]\left(2\pi r^2 X_j[mm^3]x10^3 + V_d[ml] + V'_a\right)}{R\left[\frac{atm.ml}{mmol.K}\right]T[K]} = n_i - n_j$$

where:

$$n_i - n_j = n_{aj}$$

which is the amount adsorbed in the tested sample, which plotted against the equilibrium pressure P_j provides the adsorption isotherm.

6. The Dubinin adsorption isotherm equation

The Dubinin adsorption isotherm equation can be inferred by the application of the Dubinin's Theory of Volume Filling, i.e., (where volume filling is a process which takes place by the filling of the adsorption space rather than the surface coverage), together with, the Polanyi's adsorption potential [32]. In this regard, in 1914, Polanyi created perhaps the first convincing physical adsorption model. Mijail. M. Dubinin, a former pupil of Polanyi applied this model that essentially entailed a link between the adsorption space volume, V_i, and the adsorption energy field, ε_i, (see **Figure 3**): i.e.,$\varepsilon_i = F(V_i)$, termed by Polanyi as the characteristic function, a temperature independent function. For the deduction of the Dubinin isotherm equation, the next consideration was that [33]:

Figure 3.
Polanyi adsorption model.

$$\mu_g = \mu_L + \varepsilon_i = \mu_a \tag{7}$$

In which, μ_g is the chemical potential of the gas phase adsorbate, μ_L is the chemical potential of the pure liquid adsorbate, μ_a is the adsorbed phase chemical potential, while ε_i is the potential energy of the adsorption field. Consequently, applying of Eq. (7), it is possible to demonstrate that:

$$\varepsilon_i = RT \ln\left(\frac{P_0}{P_i}\right) \tag{8}$$

where P_o is the vapor pressure of the adsorptive at the temperature, T is the adsorption experiment, while P_i is the equilibrium adsorption pressure (ε could be also designed as the differential work of adsorption). Now, following the so-called Gurvich rule, it is possible to obtain the subsequent relation $V_i = V^L n_a$ between the volume of the adsorption space, V_i, and the amount adsorbed, where V^L is the molar volume of the liquid phase that conforms to the adsorbed phase. Combining Eq. (8) with the characteristic function, the relation between the volume of the adsorption space, and the amount adsorbed, we will get [32]:

$$F(V_i) = f(n_a) = \varepsilon_i = RT \ln\left(\frac{P_0}{P_i}\right) \tag{9}$$

Now, applying the Weibull distribution function, the relation between the amount adsorbed, n_a, and the differential work of adsorption, ε, is defined by the following relation [33]:

$$n_a = N_a \exp\left(-\frac{\varepsilon}{E}\right)^n \tag{10}$$

where E is a parameter termed the characteristic energy of adsorption; meanwhile, N_a is the maximum amount adsorbed in the volume of the micropore, n ($1 < n < 5$) being an empirical parameter. Now combining Eqs. (9) and (10) is feasible to construe the Dubinin adsorption isotherm equation [32] as follows:

$$n_a = N_a \exp\left(-\frac{RT}{E} \ln\left[\frac{P_0}{P}\right]\right)^n \tag{11}$$

It is possible, as well, to express the Dubinin adsorption isotherm equation in linear form:

$$\ln(n_a) = \ln(N_a) - \left(\frac{RT}{E}\right)^n \ln\left(\frac{P_0}{P}\right)^n \tag{12}$$

which is a very powerful tool for the description of the experimental data of adsorption in microporous material.

In **Figure 4** is shown the Dubinin plot of N_2 adsorption data at 77 K in the pressure range: $0.001 < P/Po < 0.03$, in a high silica commercial H-Y zeolite, precisely, the acid Y zeolite labeled CBV-720, manufactured by PQ corporation; where, adsorption data was gathered in an Autosorb-1 automatic volumetric gas adsorption system [26]; been evidently the experimental data correctly fitted by Eq. (12)

Recapitulating, the concrete form to made the linear Dubinin plot as represented in **Figure 4** was as follows:

$$y = \ln(n_a) = \ln(N_a) - \left(\frac{RT}{E}\right)^n \ln\left(\frac{P_0}{P}\right)^n = b - mx$$

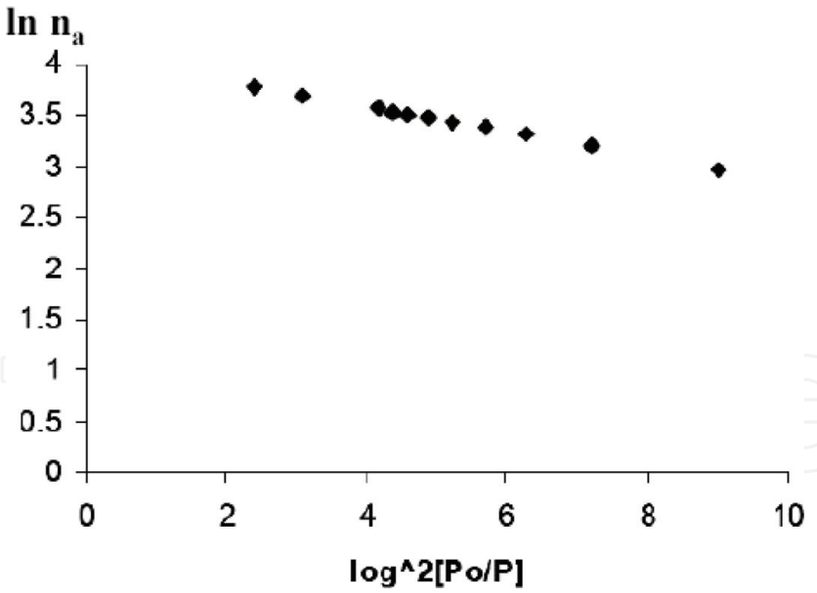

Figure 4.
Dubinin plot sample CBV-720 N_2 at 77 K [32].

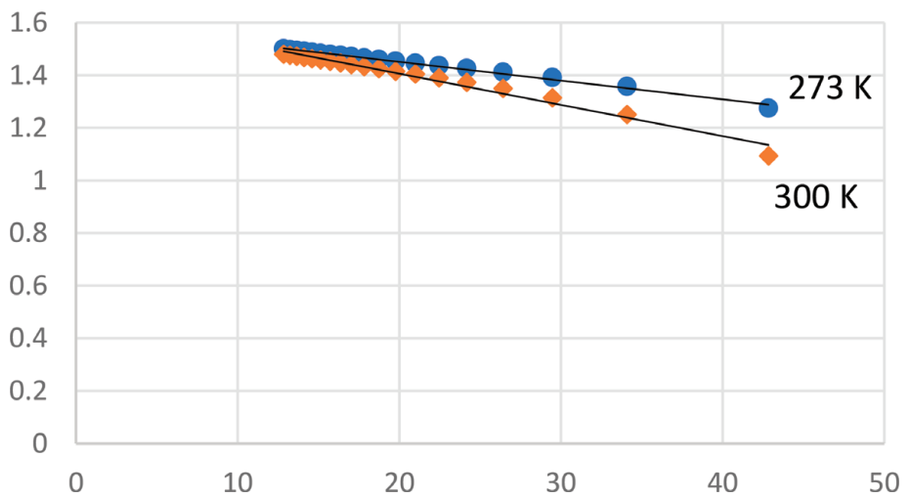

Figure 5.
Dubinin plot of carbon dioxide adsorption on nickel nitroprusside [34].

where $y = \ln(n_a)$, $b = \ln(N_a)$, $m = \left(\frac{RT}{E}\right)^n$, and $x = \ln\left(\frac{P_0}{P}\right)^n$

Nevertheless, this fitting process can be as well made using a non-linear regression method; in which, the fitting process is carried out with a program based on a least square procedure, allowing the calculation of the best fitting parameters of the Eq. (12), that is, N_a, E, been n, taken as a constant, for example, n = 2; additionally the program compute the regression coefficient, along with the standard errors.

As another example, in **Figure 4**, the use of the Dubinin equation in the measurement of the micropore volume, of a nickel nitroprusside (Ni-NP), is reported [34](**Figure 5**).

7. Osmotic and Langmuir-type adsorption isotherms

Within the frame of the osmotic theory of adsorption, the adsorption phenomenon in a microporous adsorbent, for example a zeolite, is considered as the

"osmotic" equilibrium between two solutions, i.e., vacancy plus molecules of different concentrations and the molecules in the gas phase. The solutions are formed in the micropores, and the gas phase, where the solvents are the vacancies, i.e., the vacuum [33] been, these solutions in equilibrium, in the case when one of the solutions is submerged in an external field.

Where the main supposition, made within the frame of this adsorption theory is that the role of the adsorption field could be simulated by; *Π.;* the so called "osmotic pressure" that is, the role of the energy of adsorption existing within zeolite or related materials channels and cavities, can be replicated by the pressure variation among the adsorbed and gas phases [32]; consequently, considering that the adsorption space is an inert volume; hence, the adsorption effect is produced by a virtual pressure compressing the adsorbed phase in this volume; in this case, we will have only a volume, i.e., a void adsorption space, in which an external pressure, *Π took* the role of the adsorption field [33]. Therefore, applying the hypothesizes of the osmotic theory of adsorption is feasible to affirm that the volume occupied by the adsorbate, V_a, and the vacancies, V_x, or free volume is [29] $V_a + V_x = V$; now in view of the fact that the volume occupied by an adsorbed molecule, b, and a vacancy is the same, therefore:

$$\frac{V_a}{b} + \frac{V_x}{b} = n_a + N^x = \frac{V}{b} = N_a$$

Consequently, if we multiply the previous equation by $\frac{1}{N_a}$, we obtain:

$$\frac{V_a}{N_a b} + \frac{V_x}{N_a b} = \frac{n_a}{N_a} + \frac{N^x}{N_a} = \frac{V}{N_a b} = X_a + X^x = 1$$

where X_a and. X^x correspondingly are the molar fractions of adsorbed molecules and vacancies. Then considering that the adsorption process in a micropore system can be described as an osmotic process; in which vacuum, that is, the vacancies is the solvent, whereas the adsorbed molecules is the solute [3]; hence, using the Osmosis Thermodynamics methodology applied to the above described model, it is possible to obtain the following adsorption isotherm equation [29, 32, 33]:

$$n_a = \frac{N_a K_0 P^B}{1 + K_0 P^B} \tag{13}$$

It is termed the osmotic isotherm of adsorption, or the Sips, or Bradleys isotherm equation, where this isotherm equation, fairly well, describes the experimental data of adsorption in zeolites, and other micoroporous materials; the linear form of the osmotic equation being expressed as follows:

$$y = P^B = N_a \left(\frac{P^B}{n_a}\right) + \frac{1}{K} = mx + b \tag{14}$$

where $y = P^B$, $x = \frac{P^B}{n_a}$, $m = N_a$, is the slope and $b = \frac{1}{K}$ is the intercept. Now it is necessary to state that for B = 1 the Osmotic isotherm reduces to a Langmuir-type adsorption isotherm for volume filling:

$$n_a = \frac{N_a K_{0,L} P}{1 + K_{0,L}, P}$$

In **Figure 6**, the linear plot of Eq. (14) is shown, using B = 0.5, fitting NH_3 at 300 K adsorption results in Mg-CMT, i.e., homoionic magnesium natural zeolite,

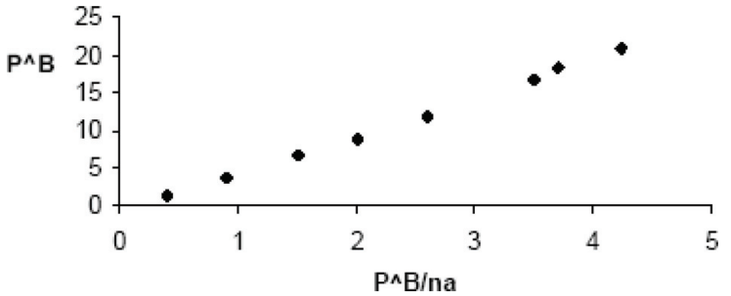

Figure 6.
Linear osmotic plot, with B = 0.5 of the adsorption data of NH_3 at 300 K in magnesium homoionic CMT zeolite [32].

concretely a blend of mordenite (39 wt. %), clinoptilolite (42 wt. %) along with additional phases (15 wt. %), where these supplementary phases are: montmorillonite (2–10 wt. %), calcite (1–6 wt. %), feldspars (0–1 wt. %), volcanic glass together with quartz (1–5 wt. %). These results were measured in a Pyrex glass volumetric adsorption vacuum system, consisting of sample holder, dead volume, dose volume, U-tube manometer, and thermostat [32]; this plot allowed us to calculate the maximum adsorption capacity of this zeolite, which is $m = N_a$ = 5.07 mmol/g, and $b = \frac{1}{K} = -0.92$, $[(\text{Torr})^{0.5}]$; as a conclusion, it is possible to affirm that the experimental data are correctly fitted by Eq. (14).

The fitting process of the osmotic isotherm equation could be also carried out with the help of a non-linear regression method, where the fitting process allows us to calculate the best fitting parameters of the Eq. (13), i.e., N_a, K_0, and B, if this parameter is not taken as a constant, for example, B = 1; besides the program calculates the regression coefficient and the standard errors.

Further adsorption isotherms are reported below [35] (**Figures 7** and **8**):

Additionally, the adsorption of oxygen (O_2) and nitrogen (N_2) in modified natural mordenite from the Palmarito, Santiago de Cuba, Cuba, deposit, composed of mordenite (80 wt.%), clinoptilolite (5 wt.%), and other phases (15 wt.%), where the other phases included montmorillonite (2–10 wt.%), quartz (1–5 wt.%), calcite (1–6 wt.%), feldspars (0–1 wt.%), and volcanic glass [2]. Labeled MP are reported in **Table 1**, where H means acid; NH, ammonia; Li, Lithium; Na, Sodium; K, Potassium; Mg, Magnesium; Ca, Calcium; Sr., Strontium; Ba, Barium zeolite; where, the oxygen nitrogen selectivity is given by [36].

$$\alpha = Y_a X_a / Y_g X_g$$

where X_a *and Ya* are the molar fractions of the adsorbates in the adsorbed phase, while X_g and Y_g are the molar fractions of both adsorbates in the gas phase.

It is necessary now to state that the framework of mordenite shows an orthorhombic unit cell displaying the space group Cmcm or Cmc21; in this sese, the unit cell of the Na cationic form has dimensions a = 18.13 Å, b = 20.49 Å, and c = 7.52 Å,

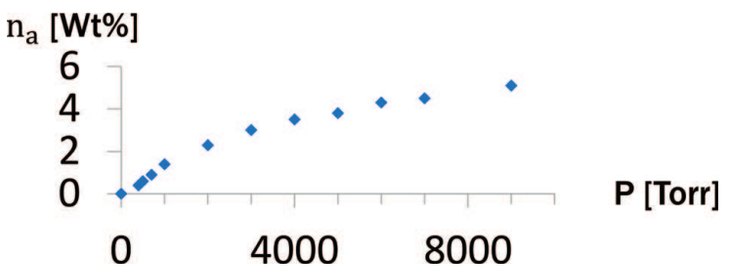

Figure 7.
Nitrogen adsorption on zeolite 5 a (Ca, Na-LTA) at 291 K.

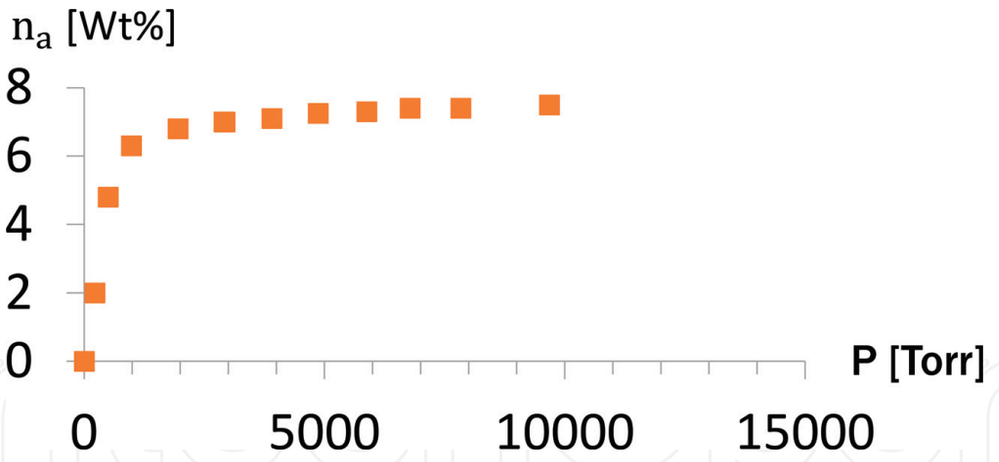

Figure 8.
Ethane adsorption on zeolite 13 X (Na-FAU) at 291 K.

ZEOLITES	$N_{MAX.OXYGEN}$ (mmol/g)	$N_{MAX.NITROGEN}$ (mmol/g)	K_{OXYGEN} $(Torr)^{-1}\times10^{-3}$	$K_{NITROGEN}$ $(Torr)^{-11}\times10^{-3}$	$\alpha_{NITROG-\ OXIG}$
H-MP	0.24	0.5	1.3	2.3	3.7
NH-MP	0.10	0.25	0.12	2.0	42
Li-MP	0.21	0.86	1.8	3.0	6.8
Na-MP	0.29	0.63	9.3	2.0	4.7
K-MP	0.07	0.26	3.1	3.7	4.4
Mg-MP	0.13	0.56	0.21	3.9	84
Ca-MP	0.27	0.56	1.4	4.8	7.1
Sr-MP	0.32	0.59	1.2	4.6	7.1
Ba-MP	0.23	0.75	1.5	1.9	4.1

Table 1.
Maximum adsorption oxygen ($N_{MAX.OXIGENO}$) and nitrogen ($N_{MAX.NITROGENO}$), Langmuir constants (K_{OXYGEN} and $K_{NITROGEN}$) and oxygen- nitrogen selectivity ($\alpha_{NITROG-\ OXIG}$) on modified natural mordenite MP [36].

along with the following composition: $Na_8Al_8Si_{40}\ O_{96} \cdot 24H_2O$; composed fundamentally of a channel system composed of a 5-membered ring system parallel to [001], having a free diameter of 6.6 Å, interconnected by smaller channels, parallel to [010], of 2.8 Å free diameter. However, the existence of stacking faults in the framework reduces the effective diameter of the channels to about 4 Å [37]. Moreover, the volume of the unit cell is $2794^{\circ}A3$, while the kinetic diameters of nitrogen and oxygen are $d_N = 3.6$ Å and $d_O = 3.5$ Å. On the other hand, the quadrupole interaction (Q) of nitrogen is larger than that of oxygen, i.e., $Q_N = 0.31$ Debye > $Q_O = 0.10$ Debye; meanwhile, the polarizability (P) of nitrogen is also bigger than that of oxygen, that is, $P_N = 4.31^{\circ}A3 > P_O = 3.96^{\circ}A3$, facts that explain the higher values measured for the Langmuir constants in the case of nitrogen in comparison with those measured for oxygen adsorption [36].

The application of the grand canonical ensemble (GCE) allows us to handle the adsorption process in microporous materials such as zeolites and related materials. In this case, the whole zeolite is considered a GCE, i.e., the zeolite cavities or channels are considered in the frame of this model as independent open systems constituting the ensemble, additionally the adsorption field within the cavities is energetically homogeneous, i.e., the adsorption field is the same at any site within

the adsorption space; besides, each cage can accommodate$m = w/b$, molecules, where w and b are the volumes of the cavity and the adsorbed molecule, respectively. Hence if the ensemble is constituted by M independent open cavities, i.e., systems, the grand canonical partition function of the zeolite is given by [32]:

where

$$\Theta = \left[1 + \lambda Z(1) + \lambda^2 Z(2) + ... + \lambda^n Z(n)\right]^M = \overline{Z}^M \tag{15}$$

$$\overline{Z} = \sum_{N=0}^{m} \lambda^N Z(N) \tag{16}$$

Is the channel or cavity grand canonical partition function; been, $Z(N)$ the Canonical Partition Function for N molecules in the channel or cavity $(0 < N < m)$, while the absolute activity is given by $\lambda = \exp(\mu/RT)$ while, μ *is* the Chemical Potential. Thereafter, as:

$$\overline{N} = \frac{\partial \ln \Theta}{\partial \lambda} = RT\left(\frac{\partial \ln \Theta}{\partial \mu}\right) \tag{17}$$

$$\theta = \frac{\overline{N}}{mM} = \frac{M\overline{N}}{Mm}\frac{\overline{N}}{m}$$

Now it is necessary to state that within the frame of the adsorption process in zeolites and related materials two cases are possible; that is, inmobile (I) or mobile (M) adsorption, been in the first and second cases, the canonical partition functions for the inmobile (Z_i) and mobile (Z_M) cases, in a homogeneous field without lateral interactions between the adsorbed molecules for $N < m$ given by:

$$Z_I(N) = \frac{m!}{N!(m-N)!}\left(Z_a^j\right)^N \exp\left(-\frac{N\left(E_0^a + \eta E_i\right)}{RT}\right) \tag{18}$$

$$Z_M(N) = \frac{w^N}{N!}(\Lambda)^N\left(Z_a^j\right)^N \exp\left(-N\left[\frac{\left(E_0 + \alpha(N/w)_i\right]}{RT}\right)\right.$$

Now since:

$$\overline{N} = \frac{\partial \ln \overline{Z}}{\partial \lambda} = \lambda\left(\frac{\partial \ln \overline{Z}}{\partial \lambda} = \frac{A}{B}\right)$$

Consequently:

$$\theta = \frac{\overline{N}}{m} = \frac{K_I P}{1 + K_I P} \tag{19}$$

$$\theta = \frac{\overline{N}}{m} = \frac{K_M P}{1 + K_{MI} P}$$

With:

$$K_I = \left[\frac{Z^j}{Z_g^j}\right]\left(\frac{1}{RT\Lambda}\right)\exp\left\{\frac{\left[E_0^g - E_0^a\right] + \Omega\theta}{RT}\right\} \tag{20}$$

$$K_M = \left[\frac{Z^j}{Z_g^j}\right]\left(\frac{b}{RT}\right)\exp\left\{\frac{\left[E_0^g - E_0^a\right] + \Phi\theta}{RT}\right\}$$

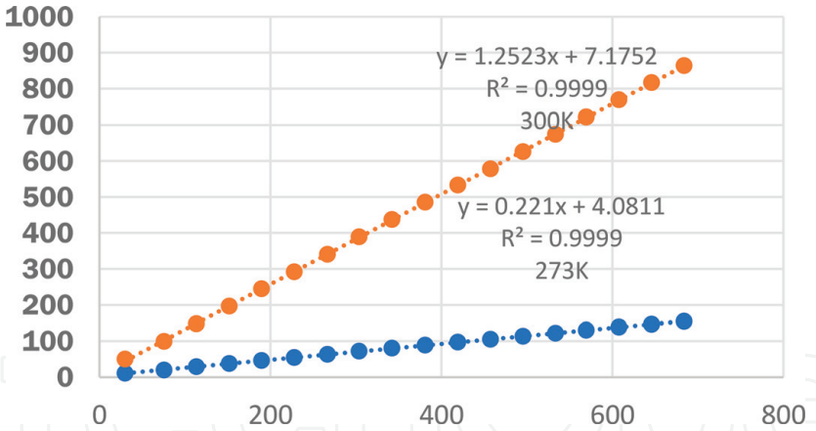

Figure 9.
Carbon dioxide adsorption on Ni-NP at 273 and 300 K [34].

Equation (19) is of the Fowler-Guggenheim type (FGT), but describing volume filling rather than surface covering, where both equations reduce to Langmuir-type (LT) isotherm equations, as well describing volume filling. Moreover, the osmotic isotherm equation and the FGT types have the same mathematical form in the case where B = 1 in the osmotic equation, as well as are equivalent to the Langmuir T type equations, when $\Omega = 0; \Phi = 0$.

To test these isotherm types, the FGT and LT type equations can be written as follows [2]:

$$\ln\left(\frac{\theta}{1-\theta}\right) = LnK + \frac{k\theta}{RT} \tag{21}$$

While the linear form of the LT type isotherms is $P = N_a(P/n_a) + 1/K = ax + b$. In **Figure 9**, the plot of carbon dioxide adsorption on Ni-NP at 273 and 300 K is reported [34].

8. t-plot method

The t-plot method suppose that the adsorbed phase as a liquid adhered film over the solid surface, the model was proposed by Halsey, De Boer, and coworkers following ideas previously proposed by Frenkel-Halsey-&-Hill which stated that it is possible to calculate, t, the width in (Angstrom) of the adsorbed layer, or multi-layer thickness [32] and plot it as a function of: $x = P/P_o$. The methodology is effective for a multilayer adsorption; in which, the surface liquid film is supposed to show a unvarying width, t, density equal to the bulk liquid adsorbate, ρ_L, and be in contact with a uniform surface that produces an attraction adsorption field over the solid surface; hence, based on the aforementioned arguments, the adsorbed amount will be [38]:

$$n_a = \rho_L t$$

Attraction by the adsorption field is given by $V(z) = \frac{A}{z^9} - \frac{B}{z^m}$. Thereafter, following a model similar to that proposed by Polanyi, where it is considered that the entropy contribution to the free energy is small in comparison with the change of enthalpy, we have $\mu - \mu_L = RT \ln\left(\frac{P}{P_0}\right)$. Hence, supposing now that [38]:

$$\mu - \mu_L = V(z) \tag{22}$$

Subsequently, since the adsorption process considered in the present model is a multilayer one, then $V(z) \approx -\frac{B}{z^m}$ and consequently $RT \ln\left(\frac{P}{P_0}\right) = -\frac{B}{z^m} = -\frac{C}{t^m}$; hence, the thickness could be evaluated after normalizing an adsorption isotherm for an adsorbent that does not possess micropores, or mesopores. Subsequently, the multiplayer thickness, t, can be calculated by the following relation:

$$t = \frac{n_a}{N_m} d_0$$

where d_0 is the thickness of a monolayer.

Thereafter, supposing again, that the surface liquid film is assumed of uniform width, t, along with having a density equal to the bulk liquid adsorbate, ρ_L, hence, we have [32]:

$$d_0 = \frac{M}{\sigma N_A \rho_L}$$

where N_A is the number of Avogado and σ is the cross-sectional area, that is, the normal area that each molecule occupies in a completed monolayer. For instance, if $\sigma(N_2)$ = 0.162 nm^2 for N_2 at 77 K, $M(N_2)$ = 28.1 g/mol, and $\rho_L(N_2)$ = 0.809 g/cm^3 then, d_0 = 0.354 nm.

The following relation *t versus*, *(1/x), is used between others* to carry out the t-plot [32, 38]:

$$t = 3.54\left(\frac{5}{2.303 \log\left(\frac{P_0}{P}\right)}\right)^{1/3} \tag{23}$$

which is the Halsey equation, valid for N_2 at 77 K or the equation used by De Boer. Moreover, the following expression:

$$t = \left(\frac{13.9}{0.034 + \log\left(\frac{P_0}{P}\right)}\right)^{1/2}$$

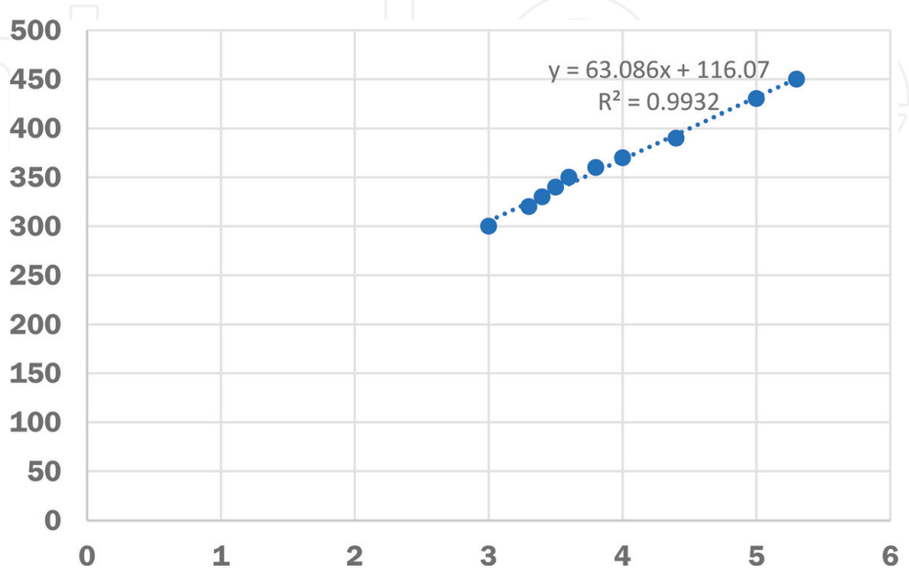

Figure 10.
t-plot for the adsorption of N_2 at 77 K in a high specific surface silica labeled 70bs-2-25C [39].

is as well used for the application of the t-plot methodology. Now it is necessary to state that the molar volume of liquid nitrogen at 77 K is $V(77K)_M^{N_2} = 32.565$ (cm^3/mol) [37].

The method to calculate, *W*, the microporous volume [in (cm^3/g)] and *S* [in (m^2/g)] the outer surface applying the t–plot method is as follows: after the elimination of the points that do not fit a linear plot (**Figure 10**):

$$y = n_a = Rt + N_a = mx + b$$

The linear regression is made, then the intercept, $b = N_a$, and the slope, $m = R$, are calculated, given that the intercept is related to the micropore volume, W^{MP}; thereafter, using the Gurvich rule $W^{MP} = N_a V_L$, where V_L, ($V(77K)_M^{N_2}$ =32.565 $\frac{cm^3}{mol}$) is the molar volume of the adsorptive at the adsorption temperature, *T*, [37] is then calculated micropore volume; $W^{MP} = 116.1x32.565 = 5.17 mmol/g_L$; together with, the outer surface, $S = RV_L = 63.08x32.565 = 2,054 m^2/g$ [39].

9. Thermodynamics of adsorption

Adsorption is a general tendency of matter, and during its occurrence, a decrease in the surface tension is experienced by the solid. For this reason, adsorption is a spontaneous process, where the Gibbs free energy decreases, i.e., $\Delta G < 0$. Besides, in the course of physical adsorption, molecules from a chaotic bulk phase are transferred to a relatively ordered adsorbed state, since in the adsorbed state molecules can only move within the surface or a pore; consequently, in the course of adsorption by the entire system, a reduction of entropy takes place, i.e., $\Delta S < 0$; subsequently [2, 32]:

$$\begin{aligned} &\Delta G = \Delta H - T\Delta S \\ &or \\ &\Delta G = \Delta H - T\Delta S < 0 \end{aligned} \tag{24}$$

Consequently, the adsorption process releases heat, i.e., it is an exothermic process. Consequently, it is stimulated by a reduction of the adsorption experiment temperature.

As a matter of fact, the main thermodynamic relation for a bulk mixture system is given by:

$$dU = TdS - PdV + \sum_i \mu_i dn_i \tag{25}$$

where S is their entropy, U is the internal energy, V is the volume, T is the temperature, μ_i is the chemical potential, and n_i is the constituent number of moles included in the system [18]. Now it is supposed that the adsorbent together with the adsorbed gas is a solid solution, labeled, system aA; thereafter, using the proposed scheme, it is possible to deduce the following equation, which thermodynamically describes the aA system [2, 32]:

$$dU_{aA} = TdS_{aA} - PdV_{aA} + \mu_A dn_A + \mu_a dn_a$$

where U_{aA}, $S_{aA,}$ and V_{aA} are the internal energy, entropy, and volume of the system aA, respectively, and μ_a and μ_A are the chemical potentials of the

adsorbate, a, and the adsorbent, A, while n_a and n_A are the number of moles of the adsorbate and the adsorbent in the system aA, respectively. Now if we define $\Gamma = n_a/n_A$; then:

$$\mu_a = \mu_a(T, P, \Gamma) \text{ and } \mu_A = \mu_A(T, P) \tag{26}$$

As a result:

$$\left[\frac{d \ln P}{dT}\right]_\Gamma = \frac{\overline{H}_g - \overline{H}_a}{RT^2} = \frac{q_{iso}}{RT^2} \tag{27}$$

where H_g and H_a are the partial molar enthalpies of the adsorbate in the gas phase and in the aA system, respectively; now, applying Eq. (16), it is possible to define the isosteric enthalpy of adsorption [31]

$$q_{iso} = \overline{H}_g - \overline{H}_a \tag{28}$$

where q_{iso} is the enthalpy of desorption, or the isosteric heat of adsorption, which is calculated with the help of adsorption isotherms. An additional significant adsorption heat is the differential heat of adsorption, since when an adsorbate contacts an adsorbent, heat is released. In our case, the thermal effect produced was measured with the help of a thermocouple placed inside the adsorbent and referred at room temperature (**Figure 11**), a variety of the Tian–Calvet heat-flow calorimeter [32]. This calorimetric methodology is characterized by the fact that the difference of temperature among the tested adsorbent and a thermostat is determined; therefore, in this heat-flow calorimeter, the produced thermal energy in the adsorption cell is permitted to flow with no limitations to the thermostat. In the calorimeter constructed by us, heat flows throughout a thermocouple; thereafter, the voltage produced by the thermocouple, which is proportional to the thermal power, is amplified and recorded in an x-y plotter (see **Figure 11**); in which, the actual thermal effect generated is the integral heat of adsorption, measured using the Eq. (2)

$$\Delta Q = k \int_0^{t_{\max}} \Delta T dt \tag{29}$$

where ΔQ is the integral heat of adsorption released during the finite increment, κ is a calibration constant, ΔT is the difference between thermostat temperature and the sample temperature during adsorption, and t is time, the differential heat of adsorption being calculated as follows [32, 33]:

$$q_{diff} = \frac{\Delta Q}{\Delta n_a} = \frac{k \int_0^{t_{\max}} \Delta T dt}{\Delta n_a}$$

The heat-flow calorimeter used consisted of the high vacuum line for adsorption measurements applying the volumetric method; as reported in **Figure 11**, the equipment comprises the following: a Pyrex glass, vacuum system including a sample holder, a dead volume, a dose volume, a U-tube manometer, and a thermostat, including now a thermocouple immersed in the adsorbent bed, which was coupled to an x-y plotter.

In **Figure 12**, the measurement of the differential heat of adsorption for the adsorption of carbon dioxide in the natural mordenite labeled MP is reported, which is a mordenite from the Palmarito, Santiago de Cuba, Cuba, deposit (mordenite (80 wt.%), clinoptilolite (5 wt.%), together with montmorillonite (2–10 wt.%), quartz (1–5 wt.%), calcite (1–6 wt.%), feldspars (0–1 wt.%), and volcanic glass) [2]. In **Figure 12**, the obtained data are shown indicating that CO_2 adsorption process in this zeolite is energetically heterogeneous; i.e., the heat of adsorption is a diminishing function of the zeolite micropore volume recovery, i.e., $\theta = n_a/n_{max}$. That is, the plot of q_{diff} versus θ shows the following: two steps, one at 90 kJ/mol and the other at 70 kJ/mol, where was released, moderately high values of the adsorption heats, indicating that CO_2 molecules powerfully interact through their quadrupole moments with the mordenite framework; after that, a reduction of

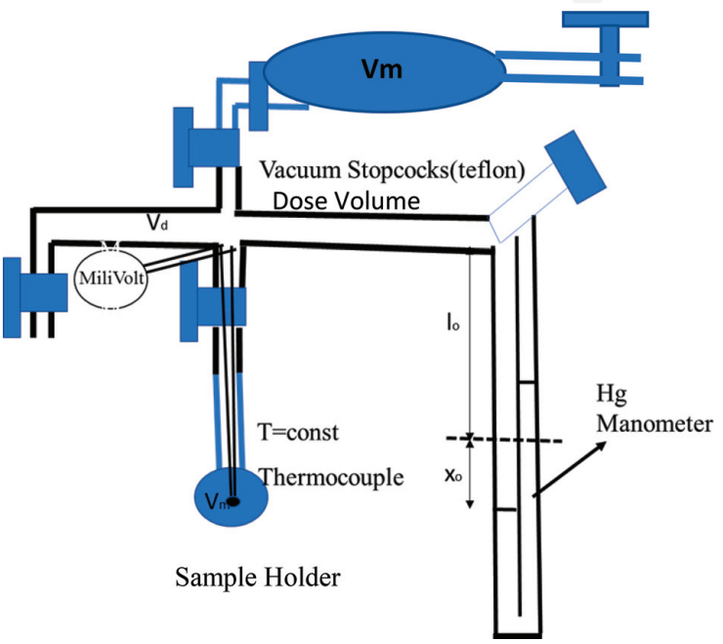

Figure 11.
Adsorption volumetric equipment.

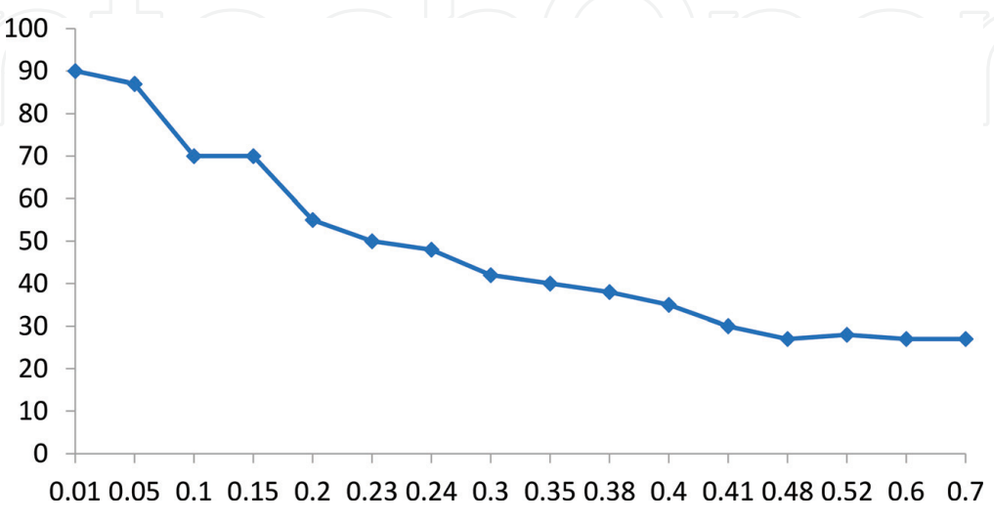

Figure 12.
Plot of q_{diff} vs. θ for the adsorption of CO_2 at 300 K in the MP zeolite [2].

the adsorption heat is found, up to a value corresponding to the bulk heat of condensation of the CO_2 molecules [26–28].

10. Adsorption interaction fields

If a molecule contacts a solid adsorbent, it is exposed to various interaction fields, such as dispersion attraction, φ_D; repulsion, φ_R; induced polarization, φ_P; permanent dipole, $\varphi_{E\mu}$; quadrupole, φ_{EQ}; and sorbate-sorbate, φ_{AA}.

Specific interactions as the acid-base interaction with the active site, φ_{AB}, if the surface contains hydroxyl bridge groups.

The dispersion or London forces among adsorbed nonpolar molecules and all types of adsorbents takes place when the transient dipoles turn out to be correlated; then, the dipoles of the nonpolar adsorbed species prompt a dipole in the atoms of the adsorbed species that act together to reduce the energy of the adsorption system. Hence, due to the correlation, the prompted dipoles created in the entire arrangement do not disappear, generating a dipole–dipole collaboration, dispersion interaction being intensity dependent on the polarizability of the adsorbate molecule and the adsorbent surface atom [40].

Additionally, the electrostatic contribution to the potential includes the dipole induced, dipole permanent and quadrupole terms, where, the induced polarization term occurs when nonpolar molecules within an electric field are polarized, and then an induced dipole moment is produced, the permanent dipole and quadrupole terms being caused by molecules whose structures produce permanent dipoles and quadrupoles; for example, H_2O, H_2S, SO_2, and NH_3 are molecules with a high dipole moment, whereas CO_2 is a molecule with a high quadrupole moment [1].

The electrostatic attractive interactions are stronger than the dispersion interactions; however, dispersion is the fundamental attractive force present during adsorption in all adsorbate-adsorbent systems, for example, in the case of molecules like H_2, Ar, CH_4, N_2, and O_2. Given that the dipole moments of these molecules are zero, the quadrupole moment is very low or absent, and the polarization effect will only be noticeable in the case of adsorbents with high electric fields; the dispersion and repulsion interactions are responsible for the adsorption effect present in all adsorption gas-solid systems; therefore, they are nonspecific interactions [2].

Author details

Rolando Roque-Malherbe[1] and Carlos de las Pozas del Rio[2*]

1 BioTECNOS Limited, Talca, Chile-San Sebastian University, Santiago, Chile

2 University San Sebastian, Santiago, Chile

*Address all correspondence to: carlos.delaspozas@uss.cl

References

[1] Breck DW. Zeolite Molecular Sieves. New York: John Wiley & Sons; 1974. pp. 635-700

[2] Roque-Malherbe R. Physical Chemistry of Materials. Energy and Environmental Applications. Boca Raton Florida: CRC Press; 2009. pp. 275-338

[3] Roque-Malherbe R. Adsorption and Diffusion in Nanoporous Materials. Boca Raton, FL, USA: CRC Press; 2018. pp. 153-287

[4] Benitez F, Travieso L, Sanchez E, Roque-Malherbe R. Waste water treatment technology. In: International Conference on Advanced Waste Water Treatment and Reclamation; September 1989; Cracow, Poland

[5] Misaelides P. Application of natural zeolites in environmental remediation. Microporous and Mesoporous Materials. 2011;**144**:15-18

[6] Wang S, Peng Y. Chemical Engineering Journal. 2010;**156**:11-24

[7] McKeen JC. Proton and ion conduction in microporous materials [Ph. D. Thesis]. Pasadena, CA, USA: California Institute of Technology; 2009

[8] Zagorodni AA. Ion Exchange Materials: Properties and Applications. Amsterdam, the Netherlands: Elsevier Science & Technology Books; 2006

[9] Lu C. Nanoporous materials chemistry. From gas separation to high pressure chemistry [Ph. D. Thesis]. Bethlehem, PA, USA: Lehigh University; 2017

[10] Caro J, Noack M. Zeolite membranes–recent developments and progress. Microporus and Mesoporous Materials. 2008;**115**:215-233

[11] Thomas JM, Thomas WJ. Principle and Practice of Heterogeneous Catalysis. New York: VCH Publishers; 1997

[12] Schlögl R. In: Ertl G, Knozinger H, Weitkamp J, editors. Preparation of Solid Catalysts. Weinheim, Germany: WileyVCH; 1999. pp. 11-28

[13] Thomas TL. Process for cation separation using zeolite materials. U. S. Patent 3,033,641; 1962

[14] McNaught AD, Wilkinson A. IUPAC Compendium of Chemical Technology. Oxford: Blackwell Scientific Publications; 1997

[15] Do JL, Friscic T. ACS Central Science. 2017;**3**:13-19

[16] Sanchez DA, Ortega N, Kumar A, Roque-Malherbe R, Polanco R, Katiyar RS, et al. Symmetries and multiferroic properties of novel room-temperature magnetoelectrics: Lead iron tantalate–Lead zirconate titanate (PFT/PZT). AIP Advances 2011;**1**:042169-1-042169-14

[17] Brinker C, Scherrer G. Introduction. In: Brinker C, Scherrer G, editors. Sol-Gel Science. 1st ed. The Physics and Chemistry of Sol-Gel Processing. New York: Academic Press; 2013. pp. 1-18

[18] Robson H, editor. Verified Synthesis of Zeolitic Materials. Amsterdam, the Netherlands: Elsevier; 2001

[19] de las Pozas C, Diaz Quintanilla D, Perez Pariente J, Roque Malherbe R, Magi M. Hydrothermal transformation of natural clinoptilolite to zeolites Y and P1: Influence of the Na, K content. Zeolites Zeolites. 1989;**9**:33-39

[20] Martens JA, Jacobs PA. Synthesis of High Silica Aluminosilicate Zeolites. Vol. 33. Amsterdam: Elsevier; 1987

[21] Gonzales E, Lariot C, Villegas R, Morales F, Cañizares H, Herrero E, et al. Influence of temperatura and syntheisis time in the acidity and morphology of ZSM-5 zeolites. Revista CENIC. 2001;**32**: 43-50

[22] Roque-Malherbe R, Lopez-Cordero R, Gonzales-Morales JA, Oñate-Martinez J, Carreras-Gracial M. A comparative study of MeAPO molecular sieves with AFI structure type. Zeolites. 1993;**13**:481-484

[23] Marsh H, Rodriguez Reynoso F. Active Carbon. Amsterdam: Elsevier; 2006

[24] Bansal RC, Gayal M. Activated Carbon Adsorption. Boca Raton, FL, USA: CRC Press-Taylor and Francis; 2005

[25] Roque-Malherbe R. Physical Chemistry of Materials. Energy and Environmental Applications. Boca Raton Florida: CRC Press; 2009. pp. 103-135

[26] Roque-Malherbe R, Lugo F, Polanco R. Applied Surface Science. 2016;**385**: 360-367

[27] Roque-Malherbe R, Carballo E, Polanco R, Lugo F, Lozano C. Structure and adsorption properties of a porous cooper hexacyanoferrate polymorph. Journal of Physics and Chemistry of Solids. 2015;**86**:65-73

[28] Roque-Malherbe R, Uwakweh ONC, Lozano C, Polanco R, Hernandez-Maldonado A, Fierro P, et al. Structural effects and interactions of carbon dioxide molecules adsorbed on Ni, Zn, and Cd nitroprussides. Journal of Physical Chemistry C. 2011;**115**: 15555-15569

[29] Roque-Malherbe R. Physical Chemistry of Materials. Energy and Environmental Applications. Boca Raton Florida: CRC Press; 2009. pp. 137-218

[30] Reguera E, delas Pozas C, Diaz Aguila C, Roque Malherbe R. Mössbauer study of hydrothermal transformation of natural clinoptilolite into Y and P1 zeolites. Journal of Solid State Chemistry. 1991;**94**:215-219

[31] Everett DH, Ottewill RH. Surface Area Determination, International Union of Pure and Applied Chemistry. London: Butterworth; 2103

[32] Roque-Malherbe R. Adsorption and Diffusion in Nanoporous Materials. Boca Raton, FL, USA: CRC Press; 2018. pp. 35-71

[33] Bering BP, Dubinin MM, Serpinskii VV. On thermodynamics of adsorption in micropores. Journal of Colloid and Interface Science. 1972;**38**:185-194

[34] Roque-Malherbe R, Lozano C, Polanco R, Marquez F, Lugo F, Hernandez-Maldonado A, et al. Study of carbon dioxide adsorption on a Cu-nitroprusside polymorph. Journal of Solid State Chemistry. 2011;**184**(5): 1236-1244

[35] Venero A, C and L Science and Technology, Hiahleah, FL, USA, Personal Communications

[36] Autie M, de las Pozas C, Balmaceda J. Revista CENIC. Ciencias Químicas. 2003;**34**:41-44

[37] Lide RD, editor. CRC Handbook of Chemistry and Physics. 88th ed. Boca Raton, Florida: Taylor & Francis Group; 2008

[38] Voogd J, Scholten JJF, Van Bekkum H. Nitrogen adsorption isotherms at 77 K have been measured of H-ZSM-5 samples. Colloids and Surfaces. 1991;**55**: 163-171

[39] Marquez-Linares F, Roque-Malherbe R. Journal of Nanoscience and Nanotechnology. 2006;**6**:1-5

[40] Roque-Malherbe R. Adsorption and Diffusion in Nanoporous Materials. Boca Raton, FL, USA: CRC Press; 2018. pp. 35-48